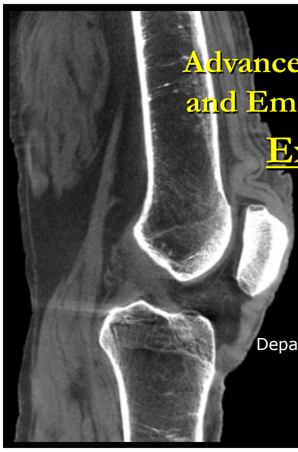

Advances in Cone-Beam CT and Emerging Applications: Extremities CBCT

W Zbijewski
Department of Biomedical Engineering
Johns Hopkins University

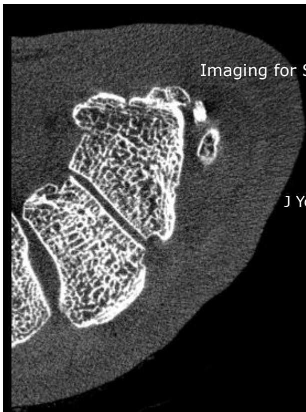

The I-STAR Laboratory
istar.jhu.edu
Imaging for Surgery, Therapy, and Radiology

JH Siewerdsen, JW Stayman,
A Sisniega, G Gang, Q Cao,
A Muhit, P DeJean, P Prakash

Carestream Health
J Yorkston, N Packard, R Senn, D Yang

JHU Radiology
JA Carrino, G Thawait, S Demehri,
M Mahesh, A. Machado

Funding Support
Carestream Health
NIH 2R01-CA-112163
NIH R21-AR-062293
NIH R01-EB-0188961

Clinical Motivation

Fracture / Trauma
→Monitoring of healing
Insufficiency fractures
- Osteoporosis
- Dietary deficiencies
- Radiation therapy
- →Need for biomarkers

Arthritis
Osteoarthritis (OA)
- ~30 million US adults
- Joint replacement
- →Need for early biomarkers

Rheumatoid arthritis
- ~1.5 million US adults
- Deformity and chronic pain
- Novel drugs
- →Monitoring of treatment response

Gout
- ~8 million US adults
- →DE imaging

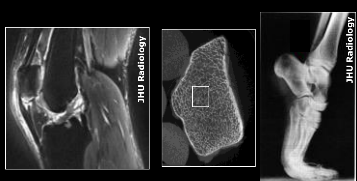

Imaging capabilities:
- Contrast resolution
  - Joint space, tendons, ligaments
- Spatial resolution
  - Bone micoarchitecure
- Bone composition (quantitative)
- Weight-bearing (functional)
- Longitudinal studies

MSK Radiology

	Contrast resolution	Spatial resolution	Quantitative	Functional (load-bearing)	Functional (motion)
Rad First line imaging	+	+++	++	+++	+
Fluoro Motion	+	++	+	++	+++
CT Trauma Fracture	++(+)	++	+++	+	++
MRI Joint internal derangement	+++	+	+		
		++	+		
		+	++		

MR – exquisite soft tissue
– limited spatial resolution

CT – high-resolution bone
– limited soft tissue

(Dual Energy-CT)

A Dedicated Extremity CBCT Scanner

System Configuration
Flat-panel detector (FPD)
Compact gantry
Sitting / standing examination

Capabilities
Weight-bearing scans
Natural stance
High isotropic spatial resolution
Multi-mode Rad / Fluoro / CBCT
Simplified logistics
Modest imaging dose
Longitudinal studies

Carestream + JHU*

Planmed Verity**

*Zbijewski et al. Med Phys 2011
*Carrino et al. Radiology 2014
**Tuominen et al. AJR 2013
** Huang et al. Skeletal Radiol 2015

Scanner Configuration

General considerations
Side entry – sliding door
Natural stance
FOV: 20 x 20 x 20 cm^3
~20 sec/scan

X-ray source and FPD
Fixed anode, 0.5 focal spot
50-125 kVp, 0.8 kW max
0.194 mm detector pixel

Clinical Prototype
Patient studies:
Weight-bearing lower extremities
Arthritis and trauma

Application Development
Joint space morphology
Bone health
Bone microarchitecture
Bone Mineral Density (BMD)

Standing Configuration

Sitting Configuration

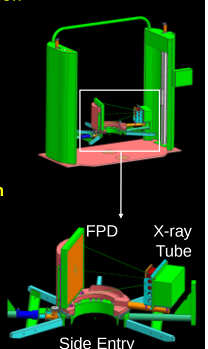

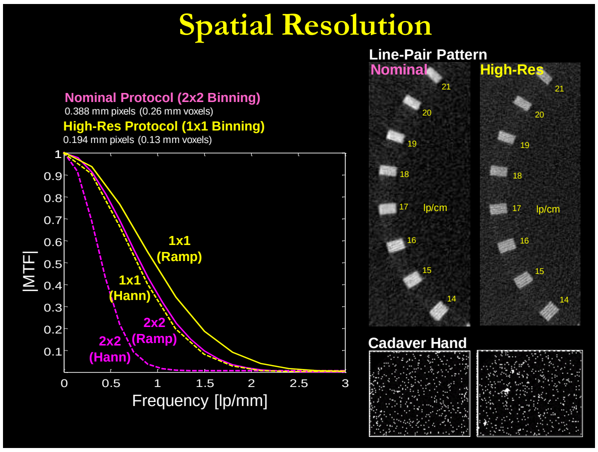
Spatial Resolution
Line-Pair Pattern
Nominal
High-Res
lp/cm
Nominal Protocol (2x2 Binning)
0.388 mm pixels (0.26 mm voxels)
High-Res Protocol (1x1 Binning)
0.194 mm pixels (0.13 mm voxels)
|MTF|
Frequency [lp/mm]
1x1 (Ramp)
1x1 (Hann)
2x2 (Ramp)
2x2 (Hann)
Cadaver Hand

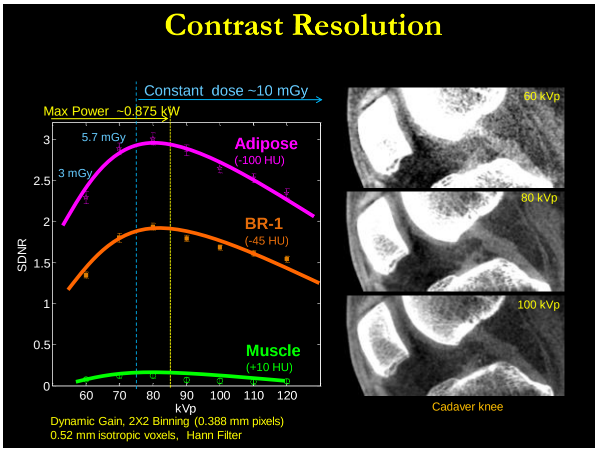
Contrast Resolution
Constant dose ~10 mGy
Max Power ~0.875 kW
5.7 mGy
3 mGy
Adipose (-100 HU)
BR-1 (-45 HU)
Muscle (+10 HU)
SDNR
kVp
Dynamic Gain, 2X2 Binning (0.388 mm pixels)
0.52 mm isotropic voxels, Hann Filter
60 kVp
80 kVp
100 kVp
Cadaver knee

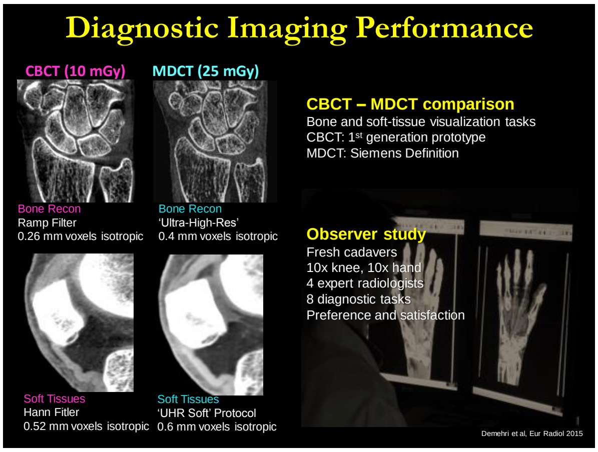
Diagnostic Imaging Performance
CBCT (10 mGy)
MDCT (25 mGy)
Bone Recon
Ramp Filter
0.26 mm voxels isotropic
Bone Recon
'Ultra-High-Res'
0.4 mm voxels isotropic
Soft Tissues
Hann Fitler
0.52 mm voxels isotropic
Soft Tissues
'UHR Soft' Protocol
0.6 mm voxels isotropic
CBCT – MDCT comparison
Bone and soft-tissue visualization tasks
CBCT: 1st generation prototype
MDCT: Siemens Definition
Observer study
Fresh cadavers
10x knee, 10x hand
4 expert radiologists
8 diagnostic tasks
Preference and satisfaction
Demehri et al, Eur Radiol 2015

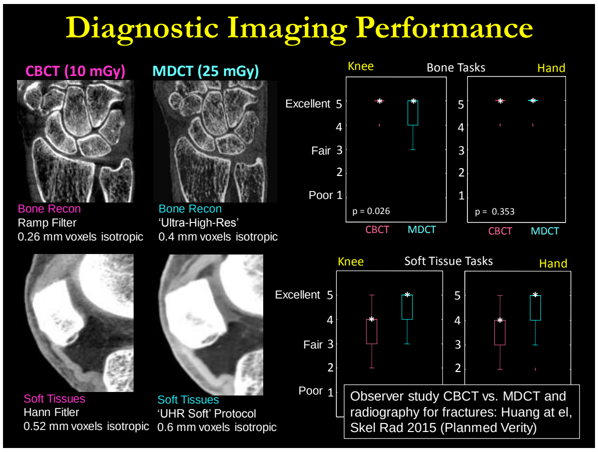
Diagnostic Imaging Performance
CBCT (10 mGy)
MDCT (25 mGy)
Bone Recon
Ramp Filter
0.26 mm voxels isotropic
Bone Recon
'Ultra-High-Res'
0.4 mm voxels isotropic
Knee
Bone Tasks
Hand
Excellent 5
4
Fair 3
2
Poor 1
p = 0.026
p = 0.353
CBCT
MDCT
Soft Tissues
Hann Fitler
0.52 mm voxels isotropic
Soft Tissues
'UHR Soft' Protocol
0.6 mm voxels isotropic
Soft Tissue Tasks
Observer study CBCT vs. MDCT and radiography for fractures: Huang at el, Skel Rad 2015 (Planmed Verity)

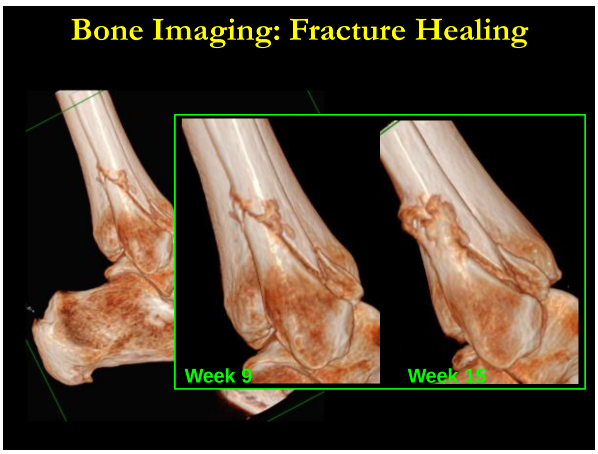
Bone Imaging: Fracture Healing
Week 9
Week 15

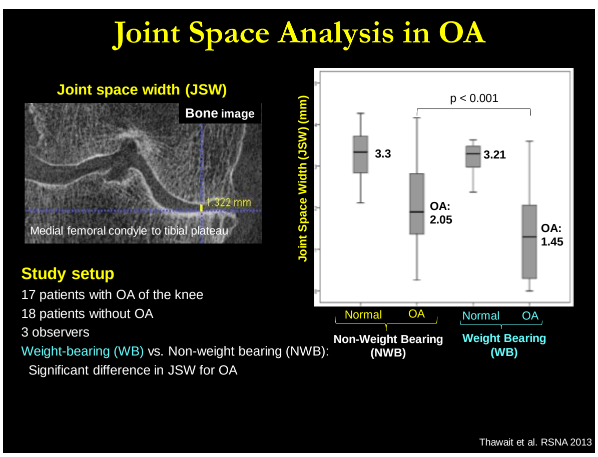
Joint Space Analysis in OA
Joint space width (JSW)
Bone image
Medial femoral condyle to tibial plateau
Study setup
17 patients with OA of the knee
18 patients without OA
3 observers
Weight-bearing (WB) vs. Non-weight bearing (NWB):
Significant difference in JSW for OA
Joint Space Width (JSW) (mm)
p < 0.001
3.3
OA: 2.05
3.21
OA: 1.45
Normal
OA
Non-Weight Bearing (NWB)
Weight Bearing (WB)
Thawait et al. RSNA 2013

Joint Space Analysis in OA

Meniscal Extrusion (ME)

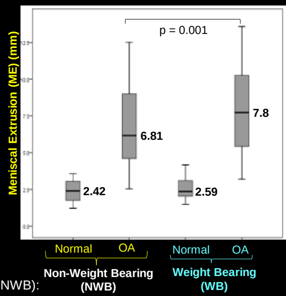

Study setup

17 patients with OA of the knee
18 patients without OA
3 observers
Weight-bearing (WB) vs. Non-weight bearing (NWB):
  Significant difference in JSW for OA
  Significant difference in ME for OA
  No significant difference in JSW or ME for non-OA

WB vs. NWB hindfoot alignement: Hirschmann at el, Eur Rad 2014 (Planmed Verity)

The Electrostatic Model

$\Phi(\partial_1\Omega) = V_1$

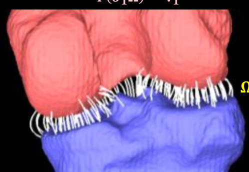

$\Phi(\partial_0\Omega) = V_0$

$\Omega \subset \mathbb{R}^2, \mathbb{R}^3$

$$\begin{cases} \vec{E} = -\nabla\Phi \\ \nabla \cdot \vec{E} = \frac{\rho}{\epsilon_0} \end{cases} \Rightarrow \nabla^2\Phi(\vec{x}) = 0 \quad \forall \vec{x} \in \Omega$$

Φ – Electric potential [V]
ρ – Charge density $[C \cdot m^{-3}]$
Ω – Joint space of interest

For an electric field $\vec{E}$ characterized by field lines $\vec{l}$ ($d\vec{l} \times \vec{E} = 0$)

$$JSW(x_0, y_0, z_0) = \int_{s_0}^{s_1} |d\vec{l}(s)|ds \quad for\ all\ (x_0, y_0, z_0) \in \partial_0\Omega$$

Cao et al Phys Med Biol 2015

Joint Space Maps

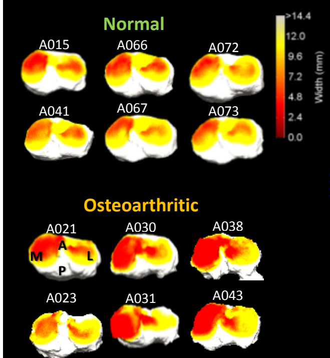

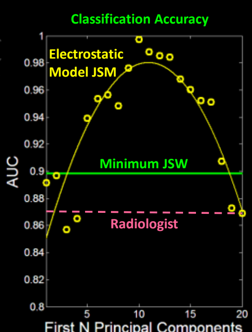

Quantitative Imaging of Bone Health

Bone health
Structure:
Micro-architecture (micro-CT)
Composition:
Bone Mineral Density BMD (DEXA / qCT)
Bone Marrow Edema BME (T2-weighted MRI)
(increased fluid content)
Risk of fracture
Mechanical competency (e.g. response to load)
Osteoporosis, arthritis, insufficiency fractures

CBCT: integrated platform for bone health assessment
Superior bone visualization to conventional CT

Micro-architecture:
High resolution required (~100 μm)
→Model-based reconstruction with deblurring
→Multi-resolution model-based reconstruction (speed)
→CMOS detectors

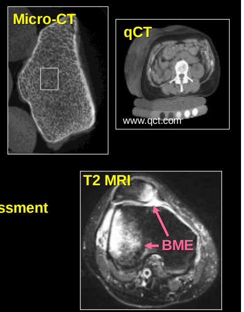

Sisniega et al, Phys. Med. Biol. (2015)

Quantitative Imaging: Microarchitecture

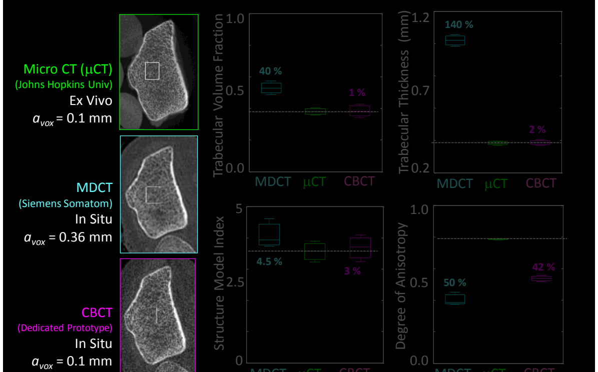

Muhit et al. SPIE 2013

Ultra-High-Resolution CBCT Imaging : Deblurring and Noise Correlations in PWLS

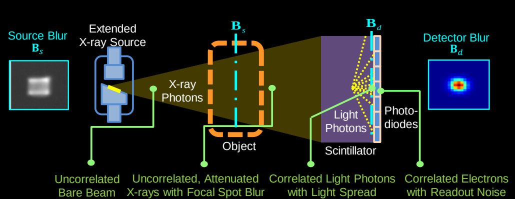

Penalized Weighted Least Squares with Deblurring and Noise Covariance:

Image Estimate

System Matrix

$$\hat{\mu} = \arg_{\mu} \min[(A\mu - l)^T K_L^{-1}(A\mu - l) + \underbrace{\beta R(\mu)}_{\text{Roughness Penalty}}]$$

Covariance Matrix:
Accounts for blur and deblurring

Deblurred line integrals

Tilley et al, Fully 3D Mtg 2015

Deblurring and Noise Correlations in PWLS

Experimental setup dominated by source blur
Deblurring the source blur introduces correlations
Modelling the correlations reduces noise in deblurred PWLS

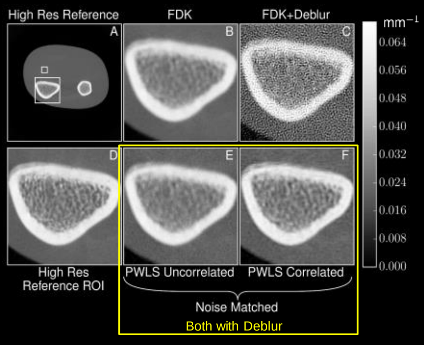

Ultra-High-Resolution CBCT Imaging : Multi-Resolution Model-Based Reconstruction

Image Estimate — System Matrix

$$\hat{\mu} = \arg_{\mu} \min[(A\mu - l)^T K_L^{-1}(A\mu - l) + \beta R(\mu)]$$

Challenges for High Resolution PWLS
System matrix A is large
20 cm FOV, <100 um Voxel Size $\Rightarrow N > 2000$

Multi-resolution PWLS
System matrix separates into:
-standard resolution component A_{STD}
-fine resolution component A_{FINE}

$$\bar{y} = I_0 \exp(-A\mu)$$
$$= I_0 \exp(A_{STD} D\{m\} \mu_S) \circ \exp(A_{FINE} \mu_F)$$

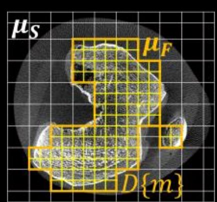

Cao et al, Fully 3D Mtg 2015

Multi-Resolution Reconstruction

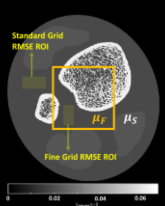

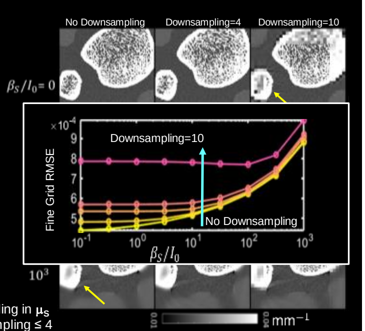

Digital Phantom Study
Fixed regularization in μ_F
Varied regularization and downsampling in μ_S
No visible artifacts in μ_F for downsampling ≤ 4

10x – 100x acceleration while maintaining quality in μ_F

Multi-Resolution Reconstruction

Knee phantom on a CBCT test-bench in extremities CBCT configuration

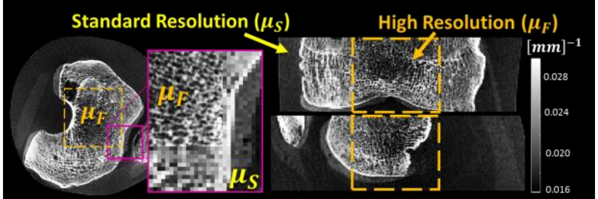

Ultra-High-Resolution CBCT Imaging : CMOS detectors

CMOS vs. aSi Flat Panel
Higher resolution (smaller pixels)
Lower electronic noise
~500 electrons/pixel
Faster read-out
30 fr/sec for 30x30 cm FOV

Experimental evaluation
600 µm CsI for CMOS and Flat Panel
Extremities CBCT configuration
0.4 focal spot x-ray tube
75 µm voxels, Ramp filter

Results and Future Work
~10-15% improvement in PSF

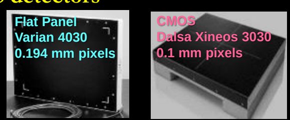

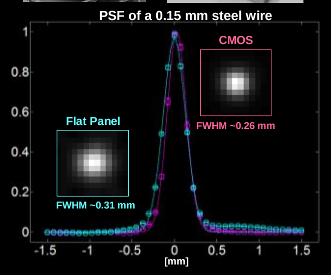

Ultra-High-Resolution CBCT Imaging : CMOS detectors

CMOS vs. aSi Flat Panel
Higher resolution (smaller pixels)
Lower electronic noise
~500 electrons/pixel
Faster read-out
30 fr/sec for 30x30 cm FOV

Experimental evaluation
600 µm CsI for CMOS and Flat Panel
Extremities CBCT configuration
0.4 focal spot x-ray tube
75 µm voxels, Ramp filter

Results and Future Work
~10-20% improvement in PSF
Better delineation of trabecular detail
CMOS limited by thick scintillator
Analytical optimization of scintillator thickness
Task-based Detectability d'

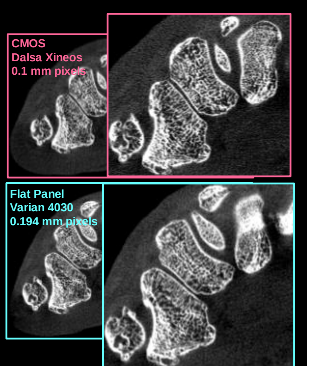

Quantitative Imaging of Bone Health

Bone health
Structure:
Micro-architecture (micro-CT)
Composition:
Bone Mineral Density BMD (DEXA / qCT)
Bone Marrow Edema BME (T2-weighted MRI)
(increased fluid content)
Risk of fracture
Mechanical competency (e.g. response to load)
Osteoporosis, arthritis, insufficiency fractures

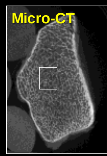

CBCT: integrated platform for bone health assessment

Bone Mineral Density / Bone Marrow Edema
Accurate attenuation values
→Comprehensive artifact correction*
BME challenging in conventional CT (partial volume from trabeculae)
Material decomposition
→Dual Energy (DE) imaging

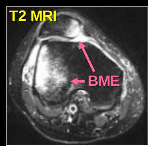

*Sisniega et al, Phys. Med. Biol. (2015)

Quantitative Imaging: BMD

BMD calculated using CBCT and MDCT (Mindways QCT)
BMD standard materials (CaHA rods) embedded in scanner door
CBCT with scatter correction

BMD calibration:
0, 75, and 150 mg/mL CaHA rods

BMD Test Phantom:
16 cm polyethylene cylinder
CaHA inserts:
0, 75, 125, 150, 250 mg/mL

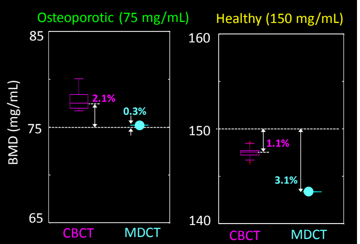

Muhit et al. SPIE 2013

Dual Energy Imaging of Bone Health

Image-based DE
Three-material decomposition
Volume preservation constraint
Volume fractions of:
Water + Fat/Marrow + Cortical Bone
Requires good image uniformity

DE Measurement of BMD
Bone fraction → BMD

DE Imaging of BME
DE: Increased water fraction=edema*

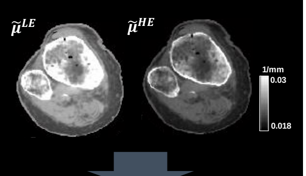

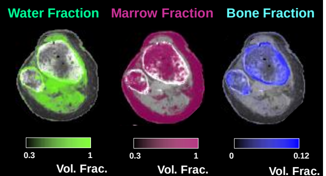

*Pache et al, Radiology (2010)

DE CBCT: Experimental Study

Tissue-Mimicking Materials[*]
Cortical Bone=Dipotassium Phosphate K_2HPO_4
Marrow/Fat=Ethanol
Edema:
Decreasing fraction of ethanol

Imaging Experiments
~10 cm diameter phantom
HE: 105 kVp, 0.1 mAs/frame, ~7 mGy CTDI
LE: 60 kVp, 0.8 mAs/frame, ~7 mGy CTDI

Artifact Correction
Fast GPU Monte Carlo scatter correction[**]
~5 min correction per scan

		Volume Composition	
Base Materials	Water	100% H_2O	
	Marrow	100% C_2H_6O	
	Cortical Bone	100% K_2HPO4	
	Bone75	75 mg/ml K_2HPO_4 in H_2O	
	Bone100	100 mg/ml K_2HPO_4 in H_20	
Edema Inserts		Marrow	Bone100
	10%	10%	90%
	25%	25%	75%
	40%	40%	60%

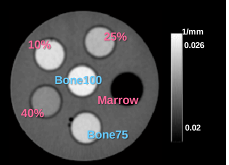

[*]Goodsitt et al, Investig. Radiol (1987)
[**]Sisniega et al, Phys. Med. Biol. (2015)

Three-Material DE Decomposition

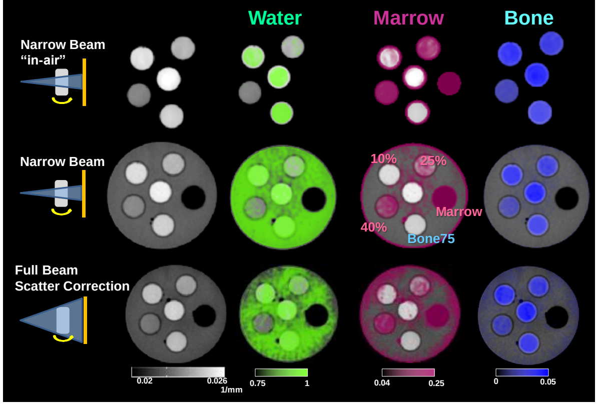

BMD Accuracy with Dual Energy CBCT

DE estimates of bone and marrow volume fractions

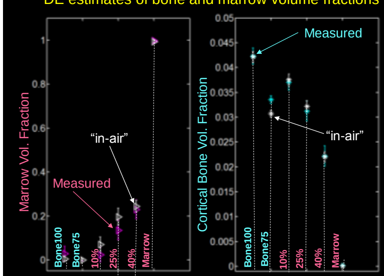

Relative difference with "in-air" narrow beam DE

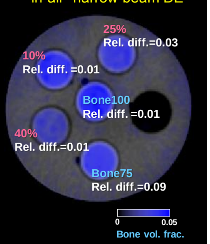

Dual Energy with Three Source CBCT

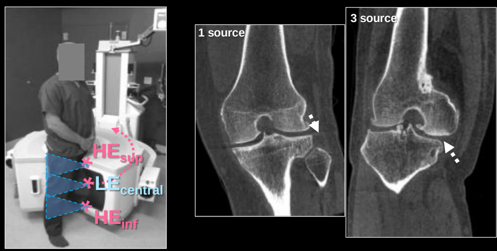

Three-Source CBCT Configuration

Custom fixed-anode unit
Three x-ray tubes arranged axially
Increased Field-of-View
Reduced cone beam artifacts
New method for Dual-Energy CBCT
Obviates need for double scan

Image Reconstruction in 3-Source DE CBCT

Penalized Likelihood (PL)

$\hat{\mu} = \arg\max_{\mu} L(\mu; y) - \beta R(\mu)$

Forward model $L(\mu; y)$
Edge-preserving Huber penalty R

Low Energy reconstruction

$L(\mu; y)$ involves LE$_{central}$ projections

High Energy reconstruction

$L(\mu; y)$ combines HE$_{sup}$ and HE$_{inf}$

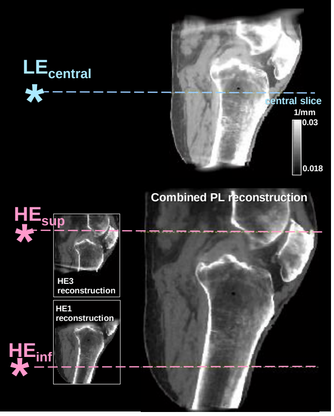

Bone and Fat Fractions in Cadaveric Knee

LE: 60 kVp, 7 mGy
HE: 105 kVp, 7 mGy
PL reconstruction

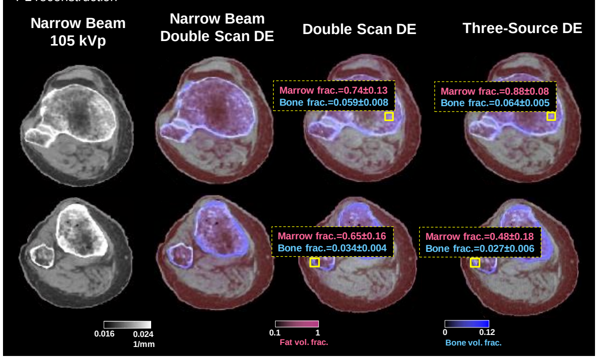

Bone and Fat Fractions in Cadaveric Knee

LE: 60 kVp, 7 mGy
HE: 105 kVp, 7 mGy
PL reconstruction

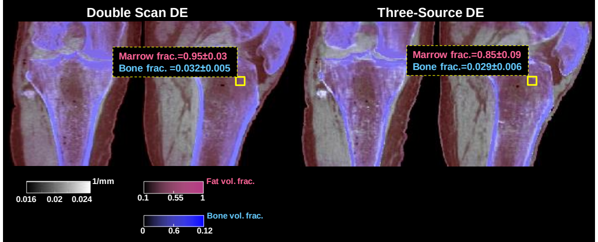

Conclusions

Extremities CBCT
Weight bearing
Soft tissue contrast
Isotropic spatial resolution (~0.5 mm)
Low dose (~10 mGy)
(~20-40 mGy for high-resolution MDCT)

Novel applications
3D Joint space maps
Quantitative imaging of bone health

Ultra-high resolution CBCT for bone morphometry
Advanced blur and noise models in PWLS
Multi-resolution PWLS
Improved delineation of trabeculae with CMOS
Scintillator optimization
Motion correction

Quantitative CBCT of bone composition
Peripheral qCT
DE imaging
BMD accuracy within 15% of "in-air" value
Detection of edema in DE CBCT
Marrow volume fraction changes ≥ 20%